Section 7

Global and regional climate models, sensitivity and impact experiments, response to external forcing

Characteristics of permafrost, total organic carbon and nitrogen distribution in Northern Eurasia

M.M. Arzhanov, S.N. Denisov, V.S. Kazantsev
A.M. Obukhov Institute of Atmospheric Physics RAS, 3, Pyzhevsky, 119017 Moscow, Russia

arzhanov@ifaran.ru

Annual-mean surface air temperature is expected to increase by 3–5 °C in Siberian region to the end of the 21st century [1]. The largest increase of precipitation rate is expected in winter for all river basins especially over northeastern part of Eurasia. It can result in changes in the thermal and hydrological conditions of permafrost [2]. Thawing of permafrost soils and increase of active layer thickness can intensify a decay of the organic matter and lead to an increase of greenhouse gases emission from soil to the atmosphere [3].

Main characteristics of permafrost are obtained using numerical scheme of heat and moisture transfer in the atmosphere-underlying surface-soil accounting for dynamics of frozen and thaw layers boundaries with water phase changes [2, 4]. External atmospheric forcing for this scheme is given for the period of 2006-2100 according to the RCP 2.6 and RCP 8.5 (Representative Concentration Pathways) anthropogenic scenarios using the global climate model IPSL-CM5A-LR from the CMIP5 (Coupled Model Intercomparison Project, phase 5) Multi-Model Database.

Assessment of seasonal active layer thickness and talik's depth (talik is part of thawed ground in the permafrost area) was performed. Annual thaw layer thickness was defined as the maximum of the seasonal thaw depth (if subsurface permafrost remains at the end of the 21st century) or the talik depth (if subsurface permafrost degrades at the end of the 21st century). The simulation results show a general increase of the annual thaw layer thickness to the end of the 21st century for the two selected scenarios. Zonal distribution analysis shows a maximum increase of the simulated thaw layer thickness at 57-61N for the RCP 2.6 scenario and at 63-67N for the RCP 8.5 for the period 2091-2100 relative to 2006-2015 (Fig. 1).

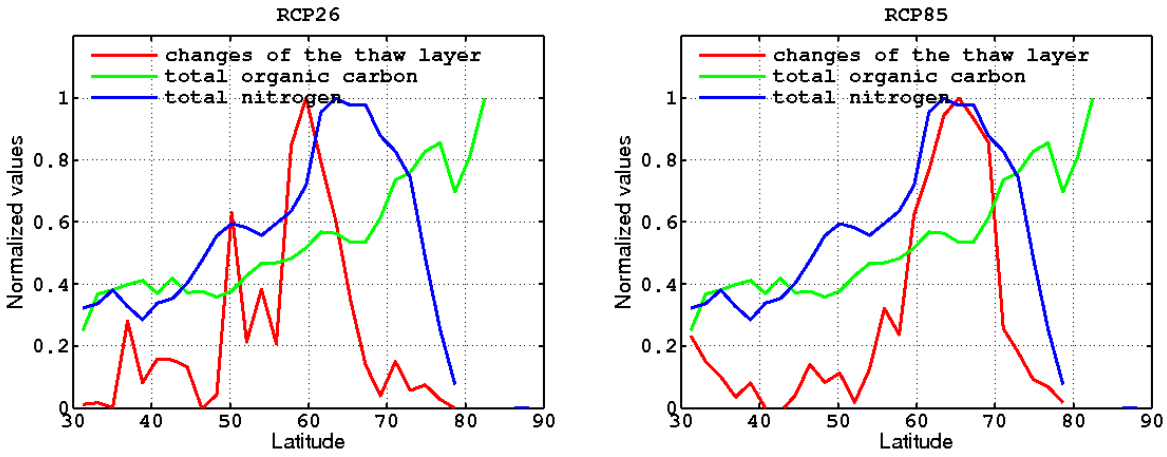

Fig. 1. Normalized changes of the simulated thaw layer thickness for the RCP 2.6 and RCP 8.5 scenarios for the period 2091-2100 relative to 2006-2015 (red line), total organic carbon distribution (green line), total nitrogen distribution (blue line) for Northern Eurasia.

In the late 21st century the simulated thaw layer thickness exceeds locally 4-6 m in the

west Siberia under RCP 2.6 scenario. In the Baikal region, the thaw layer thickness exceeds 4 m. This occurs due to the formation of taliks. Subsurface permafrost turns to a relic form in the regions near contemporary permafrost southern boundary in the Northern Eurasia. In the northern regions of central and eastern Siberia increased thawing depth does not exceed 0.4-0.6 m by the end of the 21st century. For the most aggressive anthropogenic scenario RCP 8.5, simulated near-surface permafrost degradation is located in the West and parts of Eastern Siberia. For the most aggressive scenario of anthropogenic forcing, the spatial structure of the changes of the thaw layer thickness is similar, but absolute values increase. In the late 21st century, near-surface permafrost is expected to remain in high latitudes of Central and Eastern Siberia under the both RCP 2.6 and RCP 8.5 scenarios.

An analysis of the zonal distribution of the total organic carbon (TOC) and nitrogen (TN) in the permafrost of the Northern Eurasia was carried out. The soil carbon and nitrogen stocks distribution are taken from ORNL DAAC data set (http://daac.ornl.gov/SOILS/guides/zinke_soil.html). Latitudinal distribution of total nitrogen in the Northern Eurasia is characterized by a maximum at 61-70N (Fig. 1). Maximum of the total organic carbon is in high latitudes of Northern Eurasia. Using the results of modeling the changes of the thaw layer thickness and the data on the TOC and TN distribution, estimates of the organic substance which can be included in the biogeochemical cycle by the subsurface permafrost degradation at the end of the 21st century were made. Total organic carbon changes under the process of permafrost degradation in the Northern Eurasia are estimated to be 15 GtC to the end of the 21st century while the total nitrogen increase can amount to 5 GtN for the RCP 2.6 scenario. Under the RCP 8.5 scenario these estimates are 43GtC and 18GtN respectively. Increase of the global TOC under the RCP 8.5 scenario is estimated to be about 33-114GtC to the end of the 21st century [5].

Acknowledgements

The Russian Fondation for Basic Research (12-05-01092, 12-05-33050, 13-05-10067, 13-05-00781, 11-05-00531, 11-05-00579, 12-05-91323-SIG), The program of the Earth Sciences Department of the Russian Academy of Sciences, Programs of the Russian Ministry for Science and Education (contracts 403 14.740.11.1043, 21.519.11.5004, and 8833), Russian Academy of Science 74-OK/11-4.

References

1. Groisman P.Ya., Blyakharchuk T.A., Chernokulsky A.V., Arzhanov M.M., et al. Climate Changes in Siberia. // in: Regional Environmental Changes in Siberia and Their Global Consequences (P.Ya. Groisman and G. Gutman eds.). Dordrecht: Springer. 2012. P.57-109.
2. Arzhanov M.M., Eliseev A.V., Demchenko P.F., Mokhov I.I., and Khon V.Ch. Simulation of Thermal and Hydrological Regimes of Siberian River Watersheds under Permafrost Conditions from Reanalysis Data // Izvestiya, Atmospheric and Oceanic Physics, 2008, Vol. 44, No. 1, pp. 83–89.
3. Schuur E.A.G., Bockheim J., Canadell J.G. et al. Vulnerability of Permafrost Carbon to Climate Change: Implications for the Global Carbon Cycle // BioScience. 2008. V. 58. No 8. P. 701-714.
4. Arzhanov M.M., Eliseev A.V., Mokhov I.I. A global climate model based, Bayesian climate projection for northern extra-tropical land areas // Glob. Planet. Change. 2012. V.86-87. P.57-65.
5. Schneider von Deimling T., Meinshausen M., Levermann A., et al. Estimating the permafrost-carbon feedback on global warming // Biogeosciences. 2012. V. 9. pp. 649-665.

Climate change projections in the Black Sea region based on CMIP5 model ensemble

M.M. Arzhanov[1], V.A. Semenov[1,2], I.I. Mokhov[1], A.B. Polonsky[3], I.A. Repina[1]

[1]A.M. Obukhov Institute of Atmospheric Physics RAS, 3, Pyzhevsky, Moscow, Russia
[2] Lomonosov Moscow State University, Moscow, Russia
[3]Marine Hydrophysical Institute NAS, 2, Kapitanskaya St., Sevastopol, Ukraine

arzhanov@ifaran.ru

Estimates of the future climate changes in the Black Sea region are of particular importance in light of rapidly developing infrastructure. 2014 Sochi Olympic Games, growing marine transportation, possible gas and oil exploration on the sea shelf: all these require an implemention of the growing factor of the global climate change in building strategies for social-economic development in the region. Previously, data of CMIP3 models have been used for analysis of temperature variability in the Black Sea region [1]. Here, we present some results of the analysis of anthropogenic climate change simulations for the 21st century using CMIP5 (Coupled Model Intercomparison Project, phase 5) model ensemble [2].

Some models were excluded from the analysis because they provide data only untill 2035. Selected models (23 in total) have different spatial resolutions ranging from 0.75°x0.75° to 2.8°x2.8°. Before processing, all models' data were interpolated on the same 1.0°x1.0° grid. Monthly mean data for the 21st century simulations performed under moderate anthropogenic scenario RCP 4.5 (Representative Concentration Pathways, experiment rcp45, implying 4.5W/m2 radiative forcing to the end of the 21st century) [3] were used for the analysis.

Annual and seasonal changes of temperature and precipitation have been analyzed. Due to space limitation, here we present in broad strokes only the annual means. Changes for annual mean surface air temperature (SAT) and precipitation averaged for the selected model ensemble in the Black Sea region (24-48W, 40-50N) for 2006-2100 are shown in Fig. 1. In this region the yearly mean air temperature increase amounts from 1.9° C to 2.5° C. The largest SAT increase by 2.6°C for the selected scenario is obtained in the north-eastern and south-eastern area of this region, whereas relatively moderate increase in temperature (about 1.9-2.2°C) is found in the central part of the Black Sea region (Fig. 1a) presumably due to larger thermal inertia of the Black Sea surface layer.

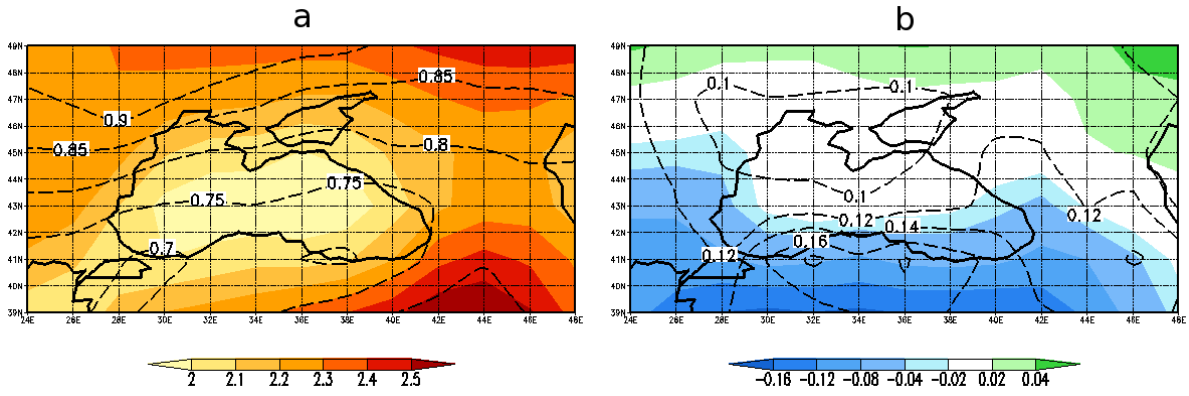

Fig. 1. Ensemble mean changes (shaded) of annual (a) surface air temperature (in °C) and (b) precipitation (in mm/day) for 2006-2100. Contours depict intra-ensemble standard deviation of the trends.

The largest increase in SAT occurs in summer in the first half of the 21st century.

Since 2070s the growth rate of the air temperature decreases. Ensemble mean temperature trends are significantly stronger than the intra-ensemble spread represented by intra-ensemble standard deviation (Fig. 1a) that increases with latitude. Precipitation only slightly changes in the selected region in 21st century (Fig. 1b). A slight increase of precipitation occurs in the northern part of the Black Sea region basically due to changes in winter season. A negative trend of annual precipitation is expected in south-west part of this region in 21st century. The intra-ensemble spread is considerably larger than the ensemble mean trends for precipitation except for the southern part of the region.

Ensemble mean and 95% confidence interval of annual SAT and precipitation for Sochi region (36-40W, 42-46N) are shown in Fig. 2. The average annual SAT increases almost linearly by about 1.5° C from 2006 to 2070 (Fig. 2a). SAT increases for all seasons in the 21st century untill 2070. The largest increase in SAT for Sochi region occurs in summer during 2006-2080 period.

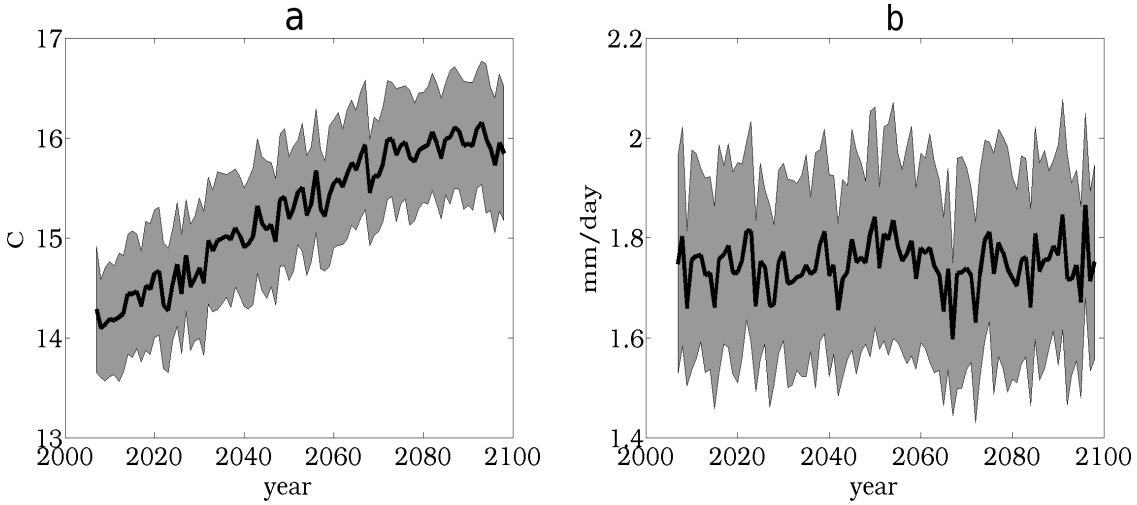

Fig. 2. Ensemble mean annual surface air temperature (a) and precipitation (b) for Sochi region (36-40W, 42-46N). Shading represents 95% confidence interval for intra-ensemble spread.

Precipitation slightly increases (by about 0.2 mm/day) in winter and decreases in summer and autumn seasons during 2006-2050 (not shown). Spring precipitation does not change during the 21st century. Ensemble mean values of annual precipitation also do not exhibit significant trend in the 21st century (Fig. 2b).

This work was supported by the Russian Foundation for Basic Research; the Presidium of the Russian Academy of Sciences (program no. 31); the Ministry for Education and Science of the Russian Federation (state contracts nos. 11.519.11.5006 and 11.G34.31.0007); and the Russian Academy of Sciences (contract no. 74_OK/11_4).

References

1. Polonsky A.B., Knyaz'kov A.S. Space-time sturcture of regional temperature field over Ukraine and Black Sea region in the global climate models. Reports of the National Academy of Sciences of Ukraine, No. 1, 1123-131, 2012 (in Russian).
2. Taylor K.E., Stouffer R.J., Meehl G.A. An Overview of CMIP5 and the experiment design. Bull. Amer. Meteor. Soc. 93, 485-498, 2012.
3. Moss R.H., Edmonds J.A., Hibbard K.A., et al. The next generation of scenarios for climate change research and assessment. Nature 463, 747-756, 2010.

Overview of the Ability of the Canadian Regional Climate Model to Simulate recent North-Eastern Pacific Tropical Cyclone Activity

Louis-Philippe Caron[1,2] Bonnie Boberg[1]
[1] *Meteorology Department, Stockholm University,* [2] *Bert Bolin Centre for Climate Research*
corresponding author: caron@misu.su.se

Introduction

In comparison with other ocean basins, and despite showing the highest cyclogenesis density, comparatively little research has been undertaken regarding tropical cyclone (TC) activity in the Eastern Pacific (EPAC). This is likely a consequence of a lack of reliable historical records and the fact that only a small portion of these storms make landfall. Interestingly enough, TC activity in the EPAC shows a downward trend over the recent past (Kossin et al., 2007), a feature unique amongst basins where TC activity is observed. Conversely, TC activity in the Atlantic is on the rise (Emanuel, 2005). The out-of-phase relationship between these two ocean basins has been discussed by (Wang and Lee, 2010).

The Canadian Global Environmental Multiscale model (GEM; Zadra et al., 2008) has been shown to produce realistic TC activity in the Atlantic (Caron et al, 2011; Caron and Jones, 2012), both in terms of geographical distribution and interannual variability. The aim of the present study is to evaluate the capability of that same model, run in three different configurations, at reproducing TC activity in the Eastern Pacific.

Three different ensembles were created for this experiment:

- Two simulations were run in limited-area mode, at 0.3° fixed resolution over a domain covering the area between the Eastern Pacific Ocean and Arabian Sea. In this configuration, the lateral boundary conditions (LBCs) were provided by ERA-40. This ensemble will be referred to as LAM-ERA.
- Three simulations were run using the same LAM domain, but in this case, the LBCs were provided by a GCM. More specifically, the LBCs originated from previous runs of GEM performed at (global) fixed resolutions of 2° (2) and 1° (1). This ensemble will be referred to as LAM-GEM.
- Two simulations were performed using a variable resolution configuration, with a 0.3° resolution domain covering the same area as the LAM domain. This ensemble will be referred to as GVAR.

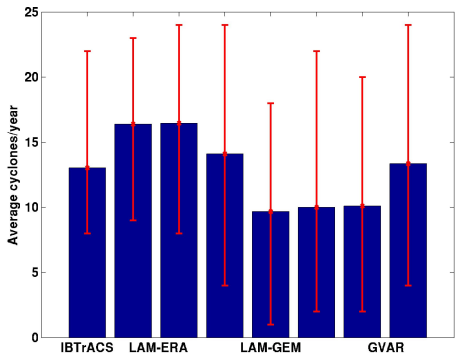

Figure 1: Average annual number of TCs for each configuration. The error bars mark the seasonal minimum and maximum.

The simulations were performed over the 1979-2006 period using observed sea surface temperature (SST) and sea-ice fraction provided by the Atmospheric Model Intercomparison Project v2 (AMIP2; Glecker, 1996) as lower boundary conditions. The TCs are tracked, using an automated procedure, during the months of June-October, inclusively. More details on the model configuration, domain and tracking procedure can be found in Caron et al. (2011). Simulated tropical cyclones are compared with historical data taken from the International Best Track Archive for Climate Stewardship (IBTrACS) database (Knapp et al., 2010).

Results

Figure 1 shows the average annual number of TCs in each of the different configurations, together with the seasonal minimum and maximum that occurred over the 28-year period. Large differences can be observed, with ERA-driven runs overestimating the activity, the LAM driven by GEM 2° showing the weakest activity and the LAM driven by GEM 1° and GVAR situated somewhere between the two. While the differences in the level of activity in the LAM configuration can be attributed to different boundary conditions, the difference in activity between the two GVAR members results from the fact that one member uses a slightly different version of the same model, one that has a slightly different lapse rate over the tropics (Caron et al., 2013).

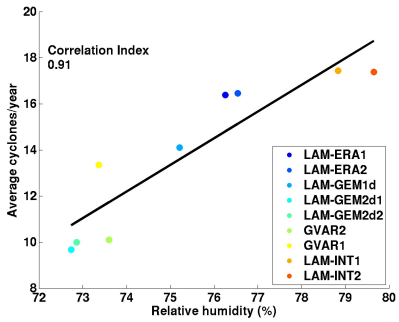

Figure 2: Relationship between mean seasonal (JAS) mid-tropospheric humidity (600 hPa) and mean number of TCs in GEM.

To understand the main factor driving the differences in the number of simulated TCs in the EPAC, the climatological values of large-scale fields known to influence cyclogenesis (Emanuel and Nolan, 2004) were computed during the most active season from July to September (JAS), over a region covering 95°-110°W and 8°-12°N of the EPAC domain. The correlation between the mean annual number of TCs and each of the individual large-scale fields was estimated. The only positive correlation was found to be between the number of TCs and the mid-tropospheric humidity at 600 hPa. This result is shown in figure 2. The correlation is very high (0.91) and significant at the 99% level.

Figure 3 shows the difference in cyclogensis density between the LAM-ERA ensemble and the LAM-GEM ensemble. Cyclogenesis in LAM-ERA is generally seen to be higher than in LAM-GEM, in agreement with figure 1. The distribution of LAM-ERA is more realistic than LAM-GEM (not shown), in large part because LAM-GEM (and GVAR) produces very few storms along the coast of Central America. This is clearly visible in figure 3. The higher cyclogenesis density over the centre of the basin and near the coast in LAM-ERA is the direct result of higher mid-tropospheric humidity (as shown in figure 2).

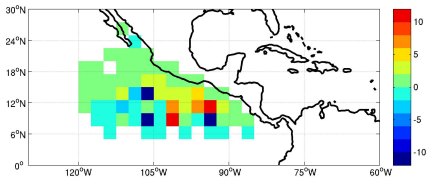

Figure 3: Difference in cyclogenesis density between the LAM-ERA ensemble and LAM-GEM ensemble. Units are number of TCs/(2.5°x2.5°)/decade.

Figure 3 also shows an area of lower cyclogenesis density in LAM-ERA (compared to LAM-GEM), between ~6°-10°N. This appears to be the result of significantly higher vertical wind shear over that region in ERA-40 driven simulations. These higher wind shear values are likely related to the difference in the representation of the ITCZ, although whether this is due to a stronger ITCZ or a shift in its mean position is unknown at this time.

Figure 4 shows the timeseries of the annual number of TCs for the LAM-ERA ensemble for the 1979-2006 period. The LAM-ERA ensemble is the only one of the three ensembles showing a significant correlation with respect to observations over the given period. The correlation coefficient for this ensemble is estimated at 0.43, which is much lower than the correlation coefficient over the Atlantic for the same ensemble, which is ~0.8. In fact, it is even lower than the correlation coeffecient of the LAM-GEM ensemble over the Atlantic, which is ~0.5. This is somewhat surprising, given that the EPAC is much closer to the lateral boundary than the Atlantic basin, which points to a reduced role of SST in modulating TC activity in that region.

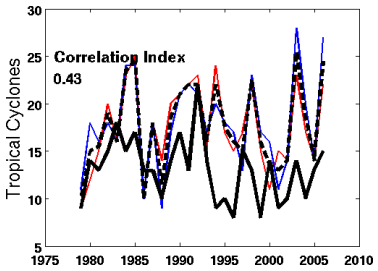

Figure 4: Timeseries of TCs for the LAM-ERA ensemble for the 1979-2006 period. Each member is in color, the ensemble mean is represented by the dash black line while the observations are represented by the full black line.

Finally, while the LAM-ERA ensemble was successful at simulating the observed upward trend in TC activity over the Atlantic, it completely fails to simulate the downward trend over the EPAC. It is not clear at this stage why this is so. Wang and Lee (2010) attributed the out-of-phase relationship between the Atlantic and the EPAC to simultaneaous variations in vertical wind shear. Given the obvious sensitivity of the model to mid-tropospheric humidity, it is possible that other large-scale fields "override" the influence of the vertical wind shear and prevent the model from capturing the downward trend. This issue is currently under investigation.

References:

Caron et al. (2013) *Clim. Dyn.*, **40**, 1257-1269. Caron and Jones (2012) *Clim. Dyn.*, **39**, 113-135. Caron et al. (2011) *Clim. Dyn.*, **5**, 869-892. Emanuel and Nolan (2004) In: 26th Conference on hurricanes and tropical meteorology, 240-241. Amer Meteorol Soc, Miami. Emanuel (2005) *Nature*, **436**, 686-688. Glecker (1996) *AMIP Newsletter*, **8**. Knapp et al. (2010) *Bull. Amer. Meteor. Soc.*, **91**, 363-376. Kossin et al. (2007) *Geophys. Res. Lett.*, **34**, 1-6. Wang and Lee (2010) *Eos Trans.*, **91**, 93-94. Zadra et al. (2008) *Physics in Canada*, **64**, 75-83.

Changes in wetland methane emissions in the IAP RAS global model under RCP anthropogenic scenarios.

S. N. Denisov, V. S. Kazantsev, M. M. Arzhanov
A.M. Obukhov Institute of Atmospheric Physics RAS

denisov@ifaran.ru

The global climate model of Institute of Atmospheric Physics of the Russian Academy of Sciences (IAP RAS CM) is extended by module of heat and moisture transport in soil [1]. Module of methane emission from wetlands [2] was improved and now takes into account carbon content in soil. The set of numerical experiments with IAP RAS CM is performed with the anthropogenic scenarios RCP for the 18th-21st centuries taking into account response of methane emissions from wetlands and the effects of chemical processes in the atmosphere to changing climate. In experiment E1 the characteristic time of methane decomposition in the atmosphere was constant. In experiments E2 and E3 it was given by temperature dependence according to the Arrhenius law and van 't Hoff equation respectively.

The IAP RAS CM generally reproduces characteristics of methane cycle in pre-industrial and modern period. Methane emission from wetlands to the atmosphere for the modern period equals to 150-160 $MtCH_4$/yr (which is consistent with observational estimates of 145±30 $MtCH_4$/yr [3]) and increasing by the end of 21st century to 170-230 $MtCH_4$/yr depending on imposed anthropogenic scenario.

Under the aggressive RCP 8.5 anthropogenic scenario concentration of methane reaches in E1 experiment 3900 ppb in the end of the 21st century (Fig. 1a). Under more moderate anthropogenic scenarios RCP 4.5 and 6.0, it reaches 1850-1980 ppb in the second half of the 21st century and decreases afterwards. Under RCP 2.6 scenario, maximum concentration of methane in the atmosphere (1730 ppb) is reached in the second decade of the 21st century. Acceleration of methane oxidation in the atmosphere due to global warming (experiments E2 and E3) reduces the growth of methane concentration by 5-40%. Related changes in the surface air temperature are rather small (less than 0.1 K globally or 4% of warming by the end of 21st century).

Although the growth of the total methane emissions amounts 10-25% it varies greatly depending on the region. Estimated growth is highest in the wetlands of Western Siberia. Simulated modern emissions for this region equal 0.5 $MtCH_4$/yr which is lesser than observational estimates of 1.5-7 $MtCH_4$/yr [4]. But the growth of emissions in 21st century amounts up to 700% depending on imposed anthropogenic scenario (Fig. 1b). This may be due not only to increasing temperature (which grows faster in high latitudes) but with increasing duration of the period of methanogenic bacteria activity in the soil.

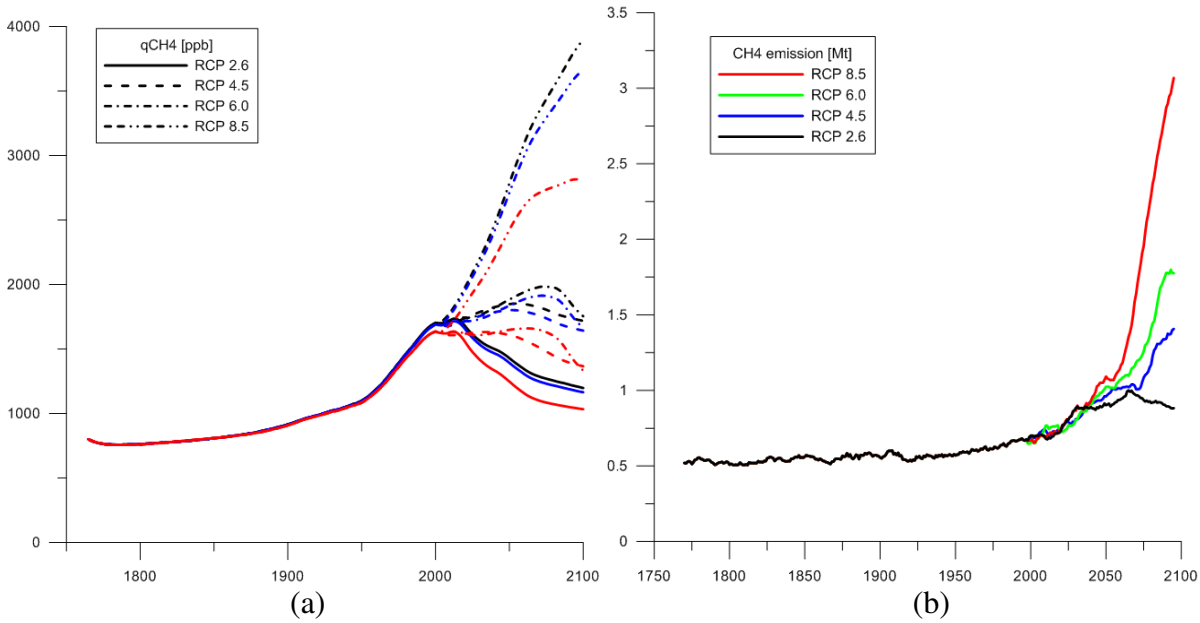

Fig. 1 Simulated concentrations of methane in atmosphere for E1 (black), E2 (blue), and E3 (red) experiments (**a**) and simulated methane emissions from Western Siberia for E1 experiment (**b**).

Acknowledgements

The Russian Foundation for Basic Research (12-05-01092, 12-05-33050, 13-05-10067, 13-05-00781, 11-05-00531, 11-05-00579, 12-05-91323-SIG), The program of the Earth Sciences Department of the Russian Academy of Sciences, Programs of the Russian Ministry for Science and Education (contracts 403 14.740.11.1043, 21.519.11.5004, and 8833), Russian Academy of Science 74-OK/11-4.

References

1. Arzhanov M.M., Eliseev A.V., Demchenko P.F., Mokhov I.I., and Khon V.Ch. Simulation of Thermal and Hydrological Regimes of Siberian River Watersheds under Permafrost Conditions from Reanalysis Data // *Izvestiya, Atmospheric and Oceanic Physics*, 2008, Vol. 44, No. 1, pp. 83–89.
2. Eliseev A. V., Mokhov I. I., Arzhanov M. M., Demchenko P. F. and Denisov S. N. Interaction of the methane cycle and processes in wetland ecosystems in a climate model of intermediate complexity // *Izvestiya, Atmospheric and Oceanic Physics*, 2008, Vol. 44, No. 2, pp. 139-152.
3. J. Lelieveld, P.J. Crutzen, and F.J. Dentener. Changing concentration, lifetime and climate forcing of atmospheric methane. *Tellus*, 50B(2):128-150, 1998.
4. Glagolev M.V. The emission of methane: ideology and methodology of «standard model» for Western Siberia // Transactions of UNESCO department of Yugorsky State University "Dynamics of environment and global climate change" / Glagolev M.V., Lapshina E.D. (eds.). – Novosibirsk: NSU. – 2008, p. 176-190. – In Russian with English Abstract.

Systematization of statement and carrying out of instrumental measurements of greenhouse gases in the tasks of forecasting with use of mathematical models

V.S. Kazantsev, S.N. Denisov, M.M. Arzhanov
A.M. Obukhov Institute of Atmospheric Physics RAS, 3, Pyzhevsky, 119017 Moscow, Russia

kazantsev@ifaran.ru

Study of the processes of emission and sink of atmospheric methane by tundra ecosystems is an important task in estimation of the contribution of natural sources in the global carbon cycle. Special actuality of this problem is connected with the expectations of significant climatic changes in the high-latitude regions of the Northern hemisphere (IPCC 2007). For the assessment of interaction of climate change and the natural ecosystems of these regions, as well as for the prediction of possible changes in the future it is necessary correspond mathematical models adequately reproduce the dynamics of the processes of emission and fixation of methane depending on the terms of the thermal and hydrological regimes of the underlying surface and the parameters of the external atmospheric impacts. Verification of such models should be carried out on joint measurements of methane emission, soil heat and hydro-physical characteristics and meteorological parameters (air temperature, precipitation, wind speed, air humidity). Proceeding from the tasks of calibration and verification of the IAP RAS model processes of temperature and moisture transfer in the ground and schemes of wetland ecosystems methane emission (Arzhanov et al., 2007; Denisov et al., 2011), carried out methodical work on choice of research sites for a full-scale measurements. The main characteristics of the sites were identified as follows:.

1. The presence at the research site dry areas of tundra and trivial tundra vegetation. This is general condition, as they occupy major part of tundra. These sites are considered as a sink of atmospheric methane.
2. The presence at the research site lakes of different types, including ice, flood and thermokarst. This requirement is presented in connection with the fact, that the genesis of lakes can indirectly influence on the intensity of methane emissions by means of difference of lake water properties (Bastviken et al., 2004).
3. The presence at the research site of wetland ecosystems. This is the most important requirement for estimation of the regional methane emission. Measurements need to get data by methane emissions from the most probable numbers of different types of wetland landscape. Estimation of regional methane emission could be obtained with methodology of the «Standard model» (Glagolev, 2008). For the most accurate estimation of methane emission from wetlands is required maximum coverage types of wetland landscapes in accordance with the classification proposed by Peregon (Peregon et al., 2009). Also, obtained data can be generalized for the study area using a dynamic model of methane emissions (Denisov et al., 2011).

Research sites were chosen using the remote sensing data. In particular, in this work were used Landsat 7TM satellite images, with high spatial resolution of 30m. (http://www.scanex.ru/ru/data/default.asp?submenu=landsat). This allows us to exactly classify types of wetland and tundra landscape. As the measurement begins in the spring season, when the underlying surface is maintained by snow cover, and there is no possibilities of on-site exactly identify the type of wetland landscape, the specific point for measurements are chosen by the satellite images. Moreover, during of experimental works the hypothesis on the maximum values of the methane emissions in the period of snow melting will be cheked on, at the basis of the data (http://aisori.meteo.ru/ClimateR) made estimates of the time for loss of snow cover for the study area (Fig. 1).

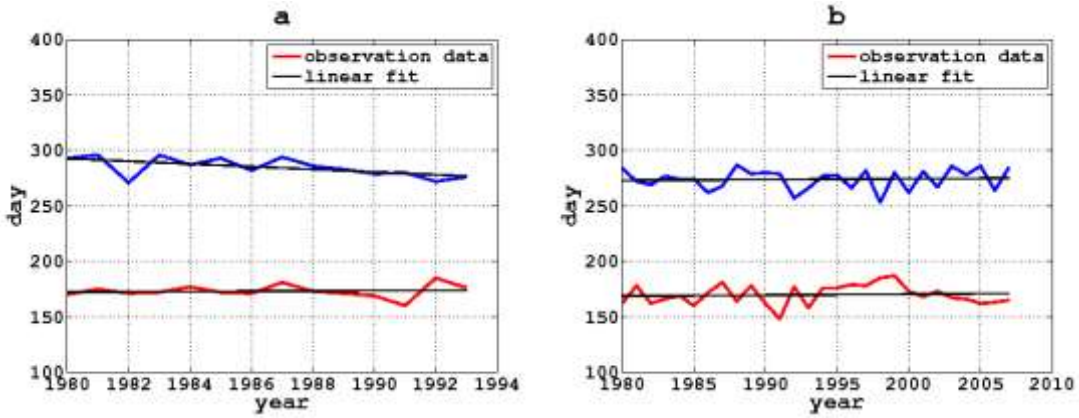

Figure 1. Interannual dynamics of periods of loss of snow cover (red line) and the formation of snow cover (blue line) by data of observations (http://aisori.meteo.ru/ClimateR) for Mis Kamennyi (a) and Dixon (b) meteostaitions. Also a linear interpolation is included for the observation (black line).

Measurements of the emissions of methane are made using a static chambers with dimming. In parallel studied environmental factors, which may influence on methane emission. For the measurement of methane emission from each type of the wetland landscape are selected few points. At each point measurements continue one day or half a day. The next day the camera is transferred to another point. Thus produces a maximum of various data sets, which gives the possibility of making the statistical processing of data and reduce the range of uncertainty in estimates of methane emissions due to the influence of ambient conditions.

Acknowledgements
The Russian Fondation for Basic Research (12-05-01092, 12-05-33050, 13-05-10067, 12-05-91323-SIG), The program of the Earth Sciences Department of the Russian Academy of Sciences, Programs of the Russian Ministry for Science and Education.

References

Bastviken D., Cole J., Pace M., Tranvik L. Methane emissions from lakes: dependence of lake characteristics, two regional assessments and a global estimate // Global Biogeochem. Cycles. 2004. V. 18. GB4009.

Glagolev M.V. 2008. The emission of methane: ideology and methodology of «standard model» for Western Siberia // Transactions of UNESCO department of Yugorsky State University “Dynamics of environment and global climate change” / Glagolev M.V., Lapshina E.D. (eds.). – Novosibirsk: NSU. – p. 176-190. – In Russian with English Abstract.

Peregon A., Maksyutov S., Yamagata Y. An image-based inventory of the spatial structure of West Siberian wetlands // Environ.Res.Lett. 2009. V.4. PP.1-6

Climate Change 2007: The Physical Science Basis. Solomon S., Qin D., Manning M. et al. (eds.). Cambridge/New York: Cambridge University Press, 2007. 996 p.

S.N. Denisov, M.M. Arzhanov, A.V. Eliseev, I.I. Mokhov. Sensitivity of methane emissions from wetland ecosystems of West Siberia to climate change: a multi-model evaluation // Atmospheric and Oceanic Optics. 2011. Vol.24. Issue. 4. pp. 319-322. – In Russian.

M.M. Arzhanov, A.V. Eliseev, P.F. Demchenko, I.I. Mokhov. Changes in the temperature and hydrological regimes near-surface permafrost modeling with the use of climatic data (reanalysis).//Earth Cryosphere. 2007. Vol.XI. Issue. 4. pp.65-69. – In Rusian.

Climate Change on small islands

Michel Déqué and Samuel Somot
Centre National de Recherches Météorologiques (CNRS/GAME), Météo-France.
42 avenue Coriolis F-31057 Toulouse Cédex 1, France, michel.deque@meteo.fr

Coupled ocean-atmosphere models regularly provide insight into the possible climate of the 21st century, warmed up by the anthropogenic greenhouse gas increase. In the next IPCC report (AR5), the CMIP5 experiment will provide a bundle of scenarios, with an average horizontal resolution of 150 km. The CORDEX project will refine the resolution by atmospheric models at 50 km resolution over large continental domains, driven by CMIP5 models at their lateral boundaries and through the sea surface temperature (sst). However, many tropical islands fall outside or too close to the border of the CORDEX domains, and the 50 km is not enough to represent them as land grid points.

The CNRM-CM5 model (Voldoire et al, 2013) is one of the contributors to CMIP5. Its sst has been used to drive, after subtraction of the monthly mean bias, a 50 km resolution version of the atmospheric component of CNRM-CM5, Arpege (Déqué, 2010). The Arpege simulations have been, in turn, used to provide lateral boundary conditions to its limited area version Aladin (Colin et al., 2010). Aladin and Arpege use here exactly the same physics and differ only by horizontal resolution. Aladin is run at 12 km resolution on small domains (typically 1000km x1000km) shown in Figure 1:

- West Indies: includes several French islands of the Caribbean Sea; we consider here Guadeloupe
- French Polynesia: we used 4 squares in the Pacific to represent the various archipelagos, but here, only the square over Tahiti is shown
- Reunion: this domain is slightly larger to include Mauritius and account for the remote effects of the high elevation of the island
- Maldives: this domain is elongated in longitude. None of the islands is resolved at 12 km, so we artificially added 3 land points, in the North, middle and South part; we consider here results for the central part (Male)
- New Caledonia: this is the only island resolved by the AGCM at 50 km. However, we consider here ocean points for Arpege to represent what CMIP5 models do

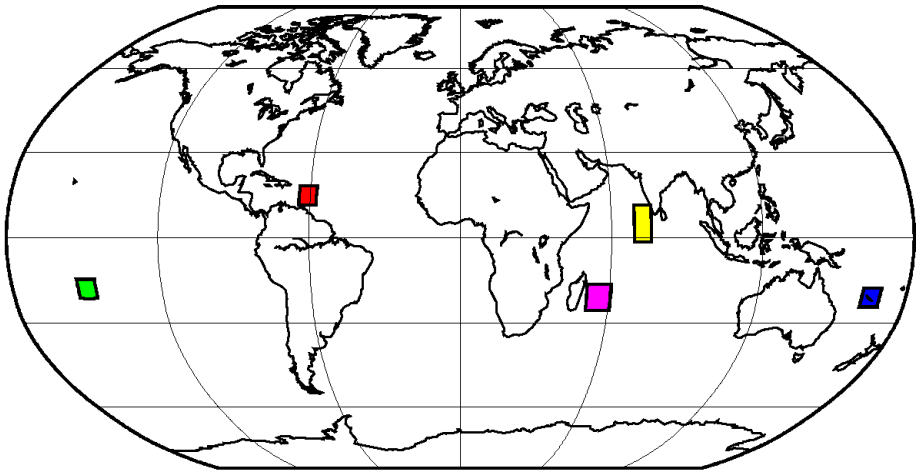

Figure 1: Location of the subdomains for ALADIN-12 km: French Polynesia (green), West Indies (red), New Caledonia (blue), Reunion Island (cyan) and Maldives Archipelago (yellow).

The question we address here is: how far can we rely on CMIP5 results to describe the climate change over our 5 islands. To reduce the uncertainty due to model sensitivity, we apply the IMPACT2C protocol, i.e. we consider the 30 year period over which the global mean temperature is 2°C above preindustrial condition (about 1.5°C above our reference 1971-2000 period). Table 1 shows that the

RCM response is warmer and drier than the GCM response. This can be easily explained by the fact that land points have the possibility to reduce the evaporation and increase temperature, compared to sea points, because of the limited soil moisture. But the RCM includes mountain which can increase precipitation by lifting the moist air masses. Table 1 shows that, beyond this average drying effect, there are strong local differences which involve the orography distribution, the large scale response, the annual cycle, and the RCP scenario. If we consider the sea points surrounding the island in the RCM (not shown), the response in 2m temperature is very close to the response in the GCM. But as far as precipitation is concerned, the response for Noumea, Male and Reunion is closer to the land point response, indicating a resolution dependence rather than an effect of soil drying.

	DJF temperature		JJA temperature		DJF precipitation		JJA precipitation	
	GCM	RCM	GCM	RCM	GCM	RCM	GCM	RCM
Tahiti RCP8.5	0.9	1.3	1.1	1.4	-12	-11	-8	-12
Tahiti RCP4.5	0.9	1.3	1.0	1.2	-9	-4	-7	-8
Guadeloupe RCP8.5	1.0	1.2	1.1	1.4	-6	-8	3	8
Guadeloupe RCP4.5	0.9	1.0	1.0	1.3	-13	-14	-2	3
Noumea RCP8.5	1.3	1.4	0.9	1.2	-2	4	-8	-30
Noumea RCP4.5	1.2	1.4	0.9	1.1	-9	-2	-8	-20
Reunion RCP8.5	1.3	1.7	1.3	1.6	25	11	9	-4
Reunion RCP4.5	1.1	1.4	1.0	1.2	11	6	4	-4
Male RCP8.5	1.2	1.4	1.3	1.3	13	-1	8	-2
Male RCP4.5	1.1	1.3	1.3	1.3	-5	-1	10	-3

Table 1: 30-year mean climate change for 2m temperature (°C) and precipitation (%) at the 5 locations for the RCP8.5 and RCP2.5 scenarios. The reference period is 1971-2000 and the scenario period is 2031-2060 (RCP8.5) and 2041-2070 (RCP4.5)

Acknowledgement : This work was supported by the European Commission (FP7-ENV/IMPACT2C) under grant 282746.

References:

Colin, J., M. Déqué, R. Radu, and S. Somot, 2010: Sensitivity study of heavy precipitations in Limited Area Model climate simulation: influence of the size of the domain and the use of the spectral nudging technique. Tellus A, 62, 591-604

Déqué, M., 2010 : Regional climate simulation with a mosaic of RCMs. Meteorologische Zeitschrift, 19, 259-266. Doi : 10.1127/0941-2948/2010/0455

Voldoire, A. E. Sanchez-Gomez, D. Salas y Mélia, B. Decharme, C. Cassou, S.Sénési, S. Valcke, I. Beau, A. Alias, M. Chevallier, M. Déqué, J. Deshayes, H. Douville, E. Fernandez, G. Madec, E. Maisonnave , M.-P. Moine, S. Planton, D. Saint-Martin, S. Szopa, S. Tyteca, R. Alkama, S. Belamari, A. Braun, L. Coquart, F. Chauvin., 2013, The CNRM-CM5.1 global climate model : description and basic evaluation , Clim. Dyn., DOI:10.1007/s00382-011-1259-y, online.

Atlantic Multidecadal Variability and hydrological cycle in the Caspian Sea watershed

V.A. Semenov [1,2], N.G. Nikitina [1,2], I.I. Mokhov [1]

[1]A.M. Obukhov Institute of Atmospheric Physics RAS, Moscow, Russia
[2] Lomonosov Moscow State University, Moscow, Russia

vasemenov@mail.ru

The Caspian Sea level (CSL) experiences large variations that highly impact society and environment. The CSL variations are determined by water cycle changes integrated over the huge (more than 3 million square km) watershed area. Volga River discharge (VRD) explains more than 80% of the CSL variations during the last century. Many different factors have been previously proposed to contribute to VRD change including major models of natural climate variability, e.g., NAO [Rodionov 1994] and ENSO [Arpe et al. 2000], and anthropogenic forcing [e.g., Arpe et al. 1999]. Recently, it has been suggested that Atlantic Multidecadal Variability (AMV), the major low-frequency climate variability mode in the North Atlantic, may strongly affect even the global climate variations [e.g., Semenov et al. 2010]. Analysis of coupled climate model simulations revealed a significant link between AMV and hydrological cycle over Eurasia on inter-decadal time scale [Mokhov et al. 2008]. Here, we focus on the AMV impact on hydrological cycle in the Caspian Sea watershed using global model simulations.

The simulations are performed using ECHAM5 atmosphere general circulation model of T31 spectral resolution (appr. 3.8° lat/lon) coupled to thermodinamical mixed layer (50 m) ocean model. The coupled model is forced by periodically (60-yr) time-varying anomalous oceanic heat convergence flux in the North Atlantic and Arctic representing AMV. The anomalous heat flux pattern, model and experimental design are described in [Semenov et al. 2010].

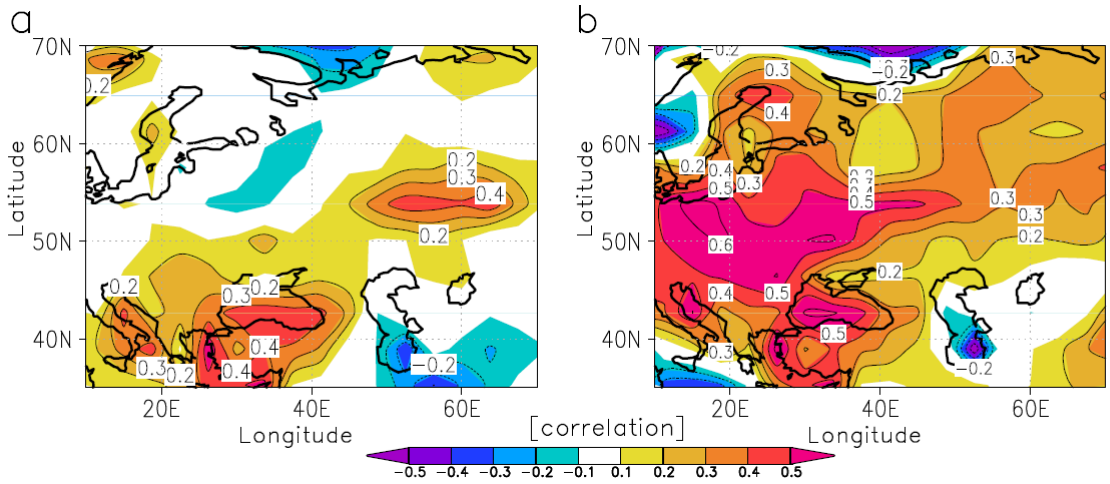

Figure 1: Correlations between simulated annual AMV SST index (see the text) and precipitation-minus-evaporation for realistic (**a**) and doubled (**b**) forcing experiments. Data have been smoothed with 15-yr running averages.

Two simulations of 500 yrs duration are performed. One uses realistic AMV amplitude (about 0.09 PW integrated heat transport). Another uses a doubled amplitude of the anomalous heat flux pattern. These simulations are idealized as they do not involve ocean dynamics and other internal variability modes essentially interacting with the AMO. From the other hand, such experiments allow one a clear separation of the AMV-related signal that is the only time-varying external forcing factor in the coupled system. The experiments start

from the present-day climate conditions (2001-2010) and maximum of the AMV forcing.

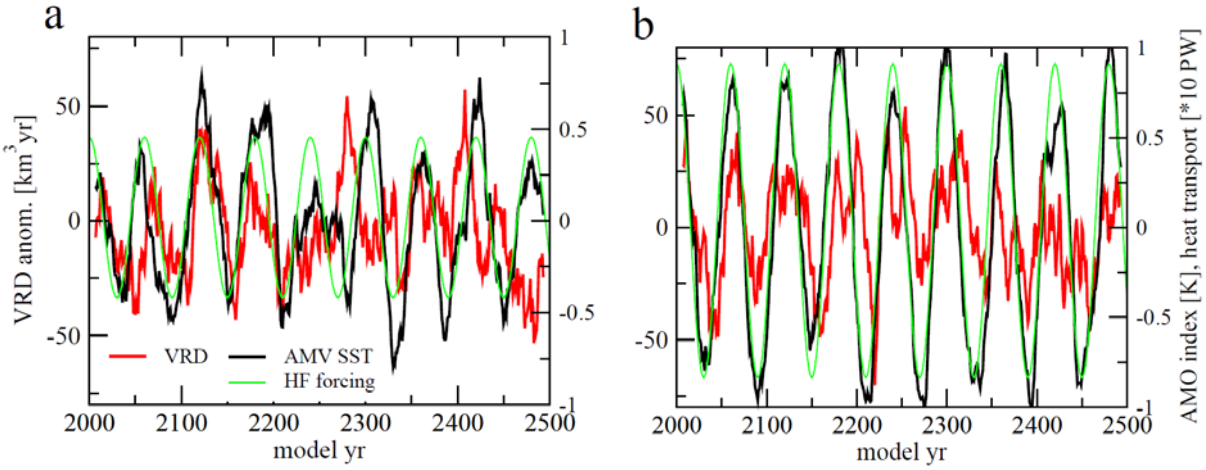

Figure 2: Simulated annual Volga River discharge anomalies (VRD, in km3/yr, red), AMV SST index (in K, black) and applied integrated heat flux (HF) forcing (in PW, green) for realistic (**a**) and doubled (**b**) forcing experiments. All time series are 15-yr running averages.

The results reveal a significant positive correlation between AMV, as represented by averaged sea surface temperature anomalies in [50W-10W,40N-60N] region, and precipitation-minus-evaporation difference over the Eastern Eurasia including Caspian Sea watershed (Fig. 1). Simulation with realistic forcing exhibits weaker correlations. However, area of stronger correlation is found in the eastern part of the Volga River watershed. Correlation of AMV SST index with precipitation is stronger for both simulations. Simulated VRD anomalies are shown in Fig. 2 together with AMV SST index and applied heat flux forcing. In doubled forcing simulation, variations of VRD are closely linked with the AMV SST index (Fig. 2b). The link is not robust in the realistic forcing simulation where periods of strong correlation (e.g. 2000-2250) and weak correlation (e.g., 2250-2350) alternate (Fig. 2a).

An estimate of the interdecadal variations of the annual Volga river discharge related to the AMV (estimated from linear regression) amounts to about 40 cubic kilometers per year which is comparable to the observed changes during the 20th century. This indicates a possible role of the AMV in driving CSL changes. The results imply a potential decadal predictability for CSL.

This work was supported by the Russian Foundation for Basic Research; the Presidium of the Russian Academy of Sciences (programs 31, 4); the Ministry for Education and Science of the Russian Federation (state contracts nos. 11.519.11.5006 and 11.G34.31.0007); and the Russian Academy of Sciences (contract no. 74_OK/11_4).

References

Arpe, K., Bengtsson, L., Golitsyn, G. S., Mokhov, I. I., Semenov, V. A., and P. V. Sporyshev (1999): Doklady Earth Sciences, 366, No. 4, 552–556.

Arpe, K., Bengtsson, L., Golitsyn, G. S., Mokhov, I. I., Semenov, V. A., and P. V. Sporyshev (2000): Connection between Caspian Sea level variability and ENSO. Geophys. Res. Lett., 27, 2693-2696.

Mokhov, I.I., Semenov, V.A., Khon, V.C., Latif, M., and E. Roeckner (2008): Connection between Eurasian and North Atlantic Climate anomalies and natural variations in the Atlantic Thermohaline Circulation based on long-term model calculations. Doklady Earth Sciences, 419A, No. 3, 502–505

Rodionov, S.N. Global and regional climate interaction: the Caspian Sea experience. 241 pp. Kluwer Academic Publ., Dordrecht, The Netherlands, 1994.

Semenov, V.A., Latif, M., Dommenget, D., Keenlyside, N.S., Strehz, A., Martin, T., Park, W. (2010): The Impact of North Atlantic-Arctic Multidecadal Variability on Northern Hemisphere Surface Air Temperature. J. Climate 23, 5668-5677.